Separation and Purification Technology 320 (2023) 124118

Contents lists available at ScienceDirect

Separation and Purification Technology

journal homepage: www.elsevier.com/locate/seppur

Optimization of the electrolytic production of Caro's acid. Towards industrial production using diamond electrodes

M.P. Castro [a], I.F. Mena [a,*], M.A. Montiel [a], J. Gäbler [b], L. Schäfer [b], C. Sáez [a], M.A. Rodrigo [a,*]

[a] Department of Chemical Engineering. Faculty of Chemical Sciences &Technologies. University of Castilla-La Mancha, Campus Universitario s/n, 13071 Ciudad Real, Spain

[b] Fraunhofer Institute for Surface Engineering and Thin Films IST, 38108 Braunschweig, Germany

ARTICLE INFO

Keywords:
Caro's acid
Process integration
Diamond anode
3-D printing

ABSTRACT

The production of oxidants to apply in different disinfection processes is of outstanding importance. Among all, peroxosulfate species, and especially the Caro's acid, are of a primary importance, because they can be stored and further electrochemically or UV-light activated for the target process, unlike other oxidants like ozone or chlorine dioxide. In this work, Caro's acid has been produced using boron-doped diamond (BDD) electrodes and an innovative tailored electrochemical cell manufactured by 3D printing. Several operating conditions like temperature, current density, and electrolyte concentration have been studied. Regarding these variables, minor improvements in the production of Caro's acid were achieved when the temperature was reduced, being more significant the improvement observed with the increase in the current density (concentration of 250 mM at 9 °C and 300 $mAcm^{-2}$ were obtained feeding 1 M of H_2SO_4). Considering the electrolyte concentration, a high concentration of sulfuric acid allowed to produce larger concentrations of Caro's acid (517 mM using 5 M of H_2SO_4), but within a matrix with more unreacted H_2SO_4. Furthermore, the process has also been conducted in divided cells (two compartments) and outstanding concentrations of around 400 mM were achieved. For operation in on-line applications, a continuous mode of production has been studied, resulting in a very predictable behavior, which is important for the future scalability of the process. Finally, a phenomenological model has been proposed and validated by fitting experimental results. This model also contributes to scale up the process and allows to fully understand and control the operational conditions and its influence on the reaction.

1. Introduction

Caro's acid is one of the most promising oxidants nowadays, with important application both in industry, where it is used for surface finishing, and in environmental remediation, where it is evaluated for the removal or organics [1,2]. Although Caro acid is a stable oxidant, i.e., it can be stored, it must be activated to improve its oxidizing conditions to make it a strong oxidant [3–7], what means that it can be preserved, which is an important advantage compared to other oxidants such as ozone or chlorine dioxide [8,9]. Its reduction product is sulphate as shown in Eq (1) and sometimes this becomes a handicap because the presence of this anion in the environment at high concentration might be disadvantageous.

$$H_2SO_5 + H_2O \rightarrow H_2SO_4 + O_2 + 2H^+ + 2e^- \quad (1)$$

Electrochemical production of Caro's acid is known for a very long time and there are patents and scientific works from the fifties of the twentieth century [10,11]. At the turn of the century, the use of diamond coatings as anode was proposed for this application and results were really promising [7,12,13]. From that moment, occasionally papers are published showing improvements in the electrochemical processes and potential applications but there is still a long way for real application of the technology [14,15].

Caro's acid can be produced electrochemically by direct exchange of electrons on the anode surface or by the action of hydroxyl radicals following the equations (2) to (3).

$$SO_4^{2-} + H_2O \rightarrow SO_5^{2-} + 2H^+ + 2e^- \quad (2)$$

$$HSO_4^{\cdot} + OH^{\cdot} \rightarrow H_2SO_5 \quad (3)$$

In addition to direct oxidation of sulfuric acid, several authors have proposed the generation of persulfate radicals by means of a reaction

* Corresponding authors.
E-mail addresses: ismael.fernandez@uclm.es (I.F. Mena), manuel.rodrigo@uclm.es (M.A. Rodrigo).

https://doi.org/10.1016/j.seppur.2023.124118
Received 21 February 2023; Received in revised form 21 April 2023; Accepted 15 May 2023
Available online 19 May 2023

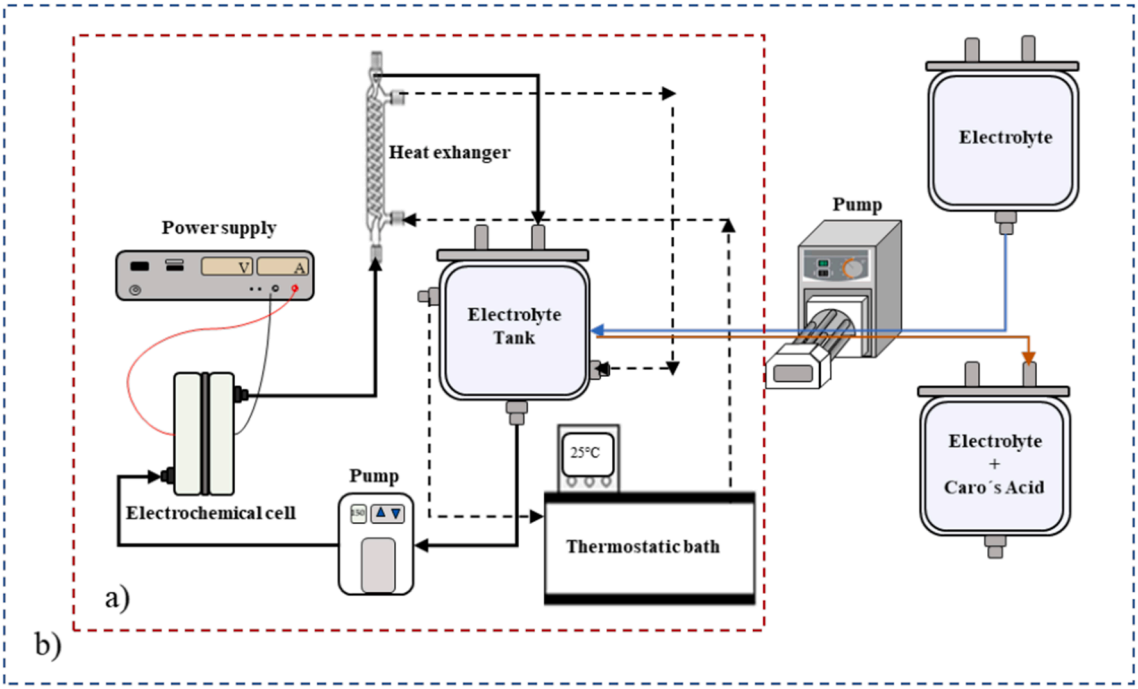

Fig. 1. Experimental set up with single compartment cell in batch (a) and continuous (b) operation mode.

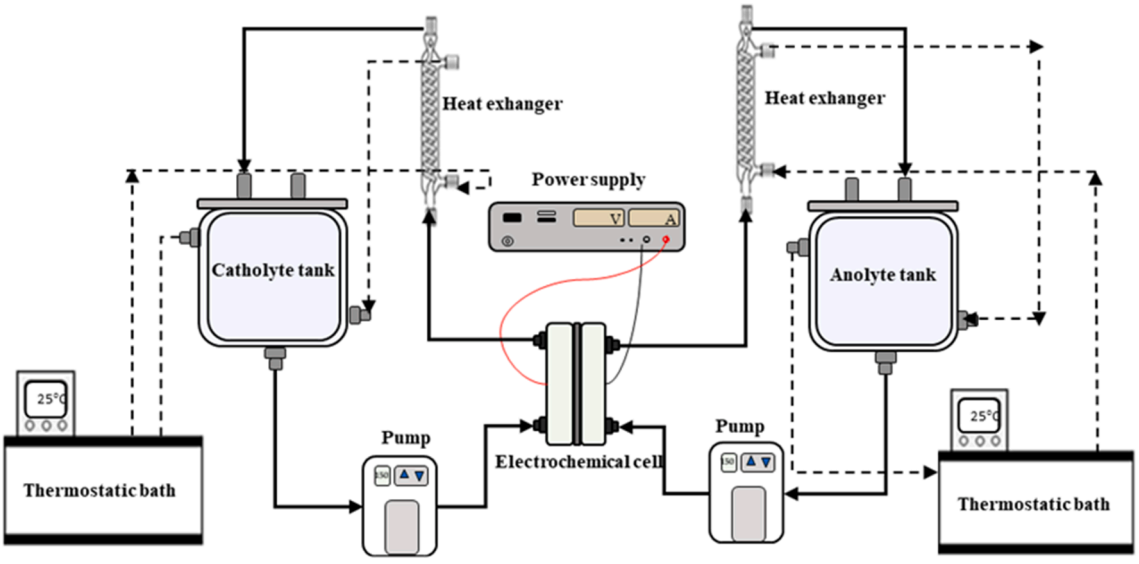

Fig. 2. Experimental set up with double compartment cell in batch operation mode.

between the HSO_4^- and the hydroxyl radicals formed in the anode surface (Eq. (4) [16].

$$HSO_4^- + \bullet OH \rightarrow SO_4^{\bullet -} + H_2O \quad (4)$$

The reduction potential of Caro's acid is 2.5 V vs SHE and this allows to be observed in voltammogram when using diamond anodes because of its extremely large electrochemical window [17,18]. As for many other oxidants produced electrochemically, the main handicap in the production is the concurrent production of scavengers in the electrolyte, among which ozone and hydrogen peroxide stand out [19–21].

With this background, this work focuses on the performance evaluation of a novel 3D printed electrochemical reactor equipped with a boron doped diamond anode, specifically designed with the aim to improve the fluid dynamics and to favor the production of Caro's acid. Several experiments were carried out to stablish the optimum variables of the process (temperature, current density, electrolyte concentration and the design of the cell) and to evaluate the feasibility of the continuous operation mode to produce Caro's acid. Moreover, a phenomenological model is proposed to predict the generation of Caro's acid depending on the variables of the electrochemical process.

2. Materials and methods

Chemicals. The main reagents involved in the experiments include sodium thiosulfate and sulfuric acid with purity of 96%, purchased by Scharlab. Potassium iodide was provided by Honeywell and sodium sulfate from PanReac Applichem. All solutions were prepared with ultrapure water from Milli-Q system.

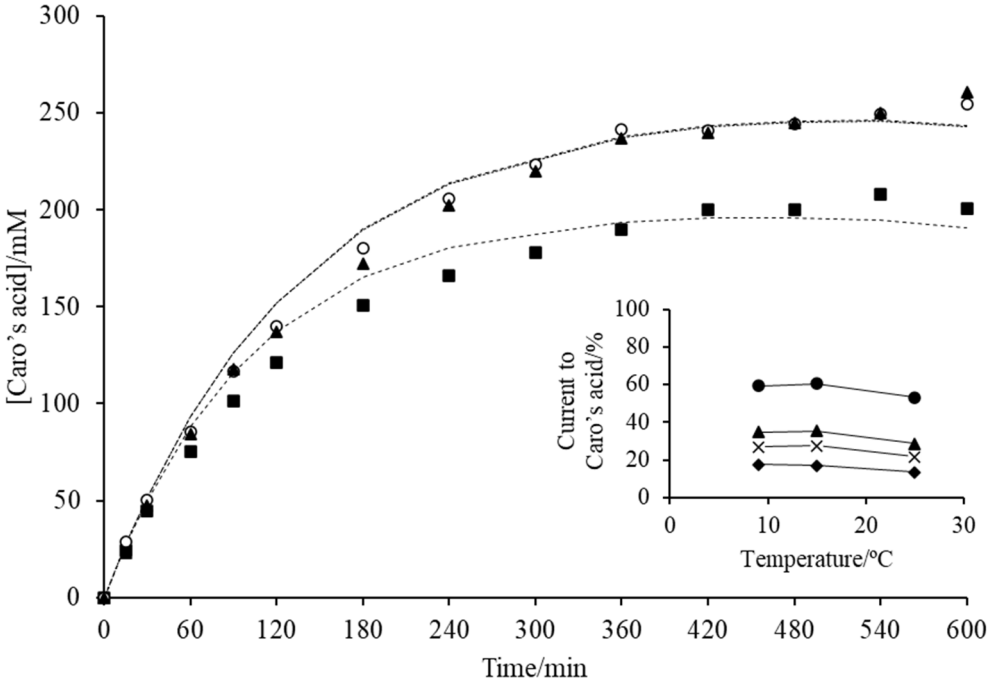

Fig. 3. Electrogeneration of Caro's acid at 9 °C (▲), 15 °C (○),25° C (■). Modelling data dashed line 1. Insert: Percentage of current used to generate Caro's acid at different electrolysis time: 1 h (●),4h (▲),6h (×),10 h (◆). Current density: 300 mA cm^{-2}, electrolyte: 1.0 M H_2SO_4.

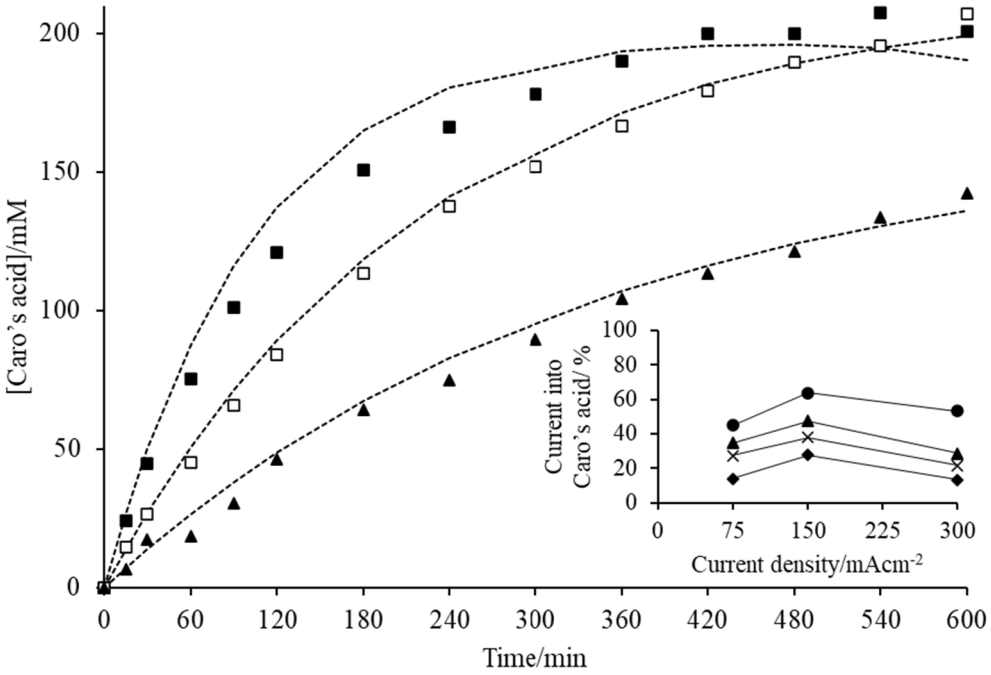

Fig. 4. Electrogeneration of Caro's acid at 300 mA cm^{-2} (■),150 mA cm^{-2} (□),75 mA cm^{-2}(▲). Modelling data: dashed line. Insert: Percentage of current used to generate Caro's acid at different electrolysis time: 1 h (●),4h (▲),6h (×),10 h (◆). T: 25 °C, electrolyte: 1 M H_2SO_4.

Analytical procedures. Analysis of total oxidants was performed by mixing the sample with excess KI and further titration of the iodine formed based on the iodometric titration method, as described in [22]. This technique quantifies by potentiometric titration with thiosulphate (0.01 N) in acidic media all the oxidants capable of oxidizing I^- to I_3. The potentiometric titration equipment used was 702 SM Titrino by Metrohm. The value obtained corresponds to an oxidant cocktail formed mostly by Caro's acid and its protonated forms. To determine the value of other species, H_2O_2 concentration was measured by spectrophotometric method, following the concentration of the complex formed between H_2O_2 and Ti^{4+} [23] obtaining near-0 values for all the samples tested. Ozone solubility is comparatively low and its contribution to the oxidants measured negligible [20].

Electrochemical measurements. The electrochemical measurements were carried out on an Autolab potentiostat/galvanostat (PGSTAT-302 N) and Booster10A. Boron doped diamond (BDD) was used as working electrode (2.25 cm^2), paper carbon and Ag/AgCl electrodes were used as counter and reference electrode, respectively. Cyclic

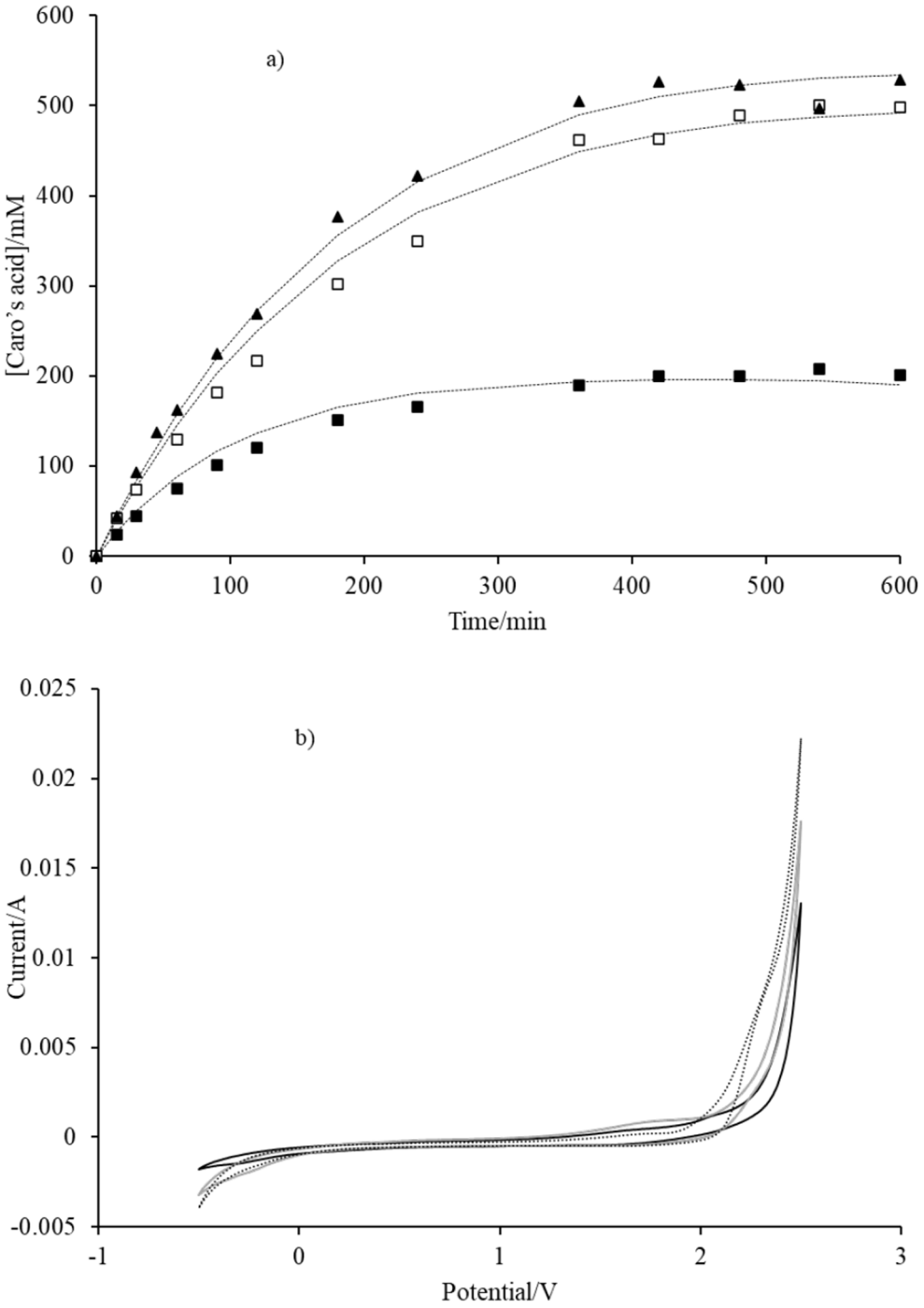

Fig. 5. a) Electrogeneration of Caro's acid at 1 M H_2SO_4 (■), 3 M H_2SO_4 (□), 5 M H_2SO_4 (▲). Modeling data: dashed line. b) Cyclic voltagrammogran with BDD electrodes in different acid sulfuric concentrations: — 1 M H_2SO_4, — 3 M H_2SO_4, 5 M H_2SO_4.

voltammetry was performed to the BBD electrodes in half-cell until stable profiles have been obtained with a scan rate 50 $mV{\cdot}s^{-1}$ with operating window between −0.5 – 2.5 V vs. Ag/AgCl.

To manufacture the boron-doped diamond (BDD) electrodes, square-shaped niobium plates with 50 mm width and length and two millimetres thickness were coated via hot-filament activated chemical vapor deposition (CVD), using a large-scale CVD reactor, designed by Fraunhofer IST, with a coating area of 500 mm × 1000 mm and a maximum electrical power of 80 kW [24]. Filament diameter was 0.5 mm. Before coating, the substrates were pre-treated by sandblasting, cleaning in de-ionised water and seeding by dipping 5 min in a suspension of nanometre-sized diamond particles in water. The carbon precursor gas was methane in a concentration of 1.83 vol-% in an excess of hydrogen. Total gas pressure was 20 mbar. The diamond layer was doped during the deposition by adding 0.49 vol % trimethylborane to achieve the necessary electrical conductivity at a boron concentration of about 2500 ppm. The electrodes were coated twice for 40 h on each side. The substrate temperature was app. 950 °C. The microcrystalline diamond layer had a film thickness of app. 7 μm.

Caro's acid electrochemical Synthesis. The 3-D printed cell was used as a single compartment cell and as double compartment cell and its details are shown in the Supplementary material section.

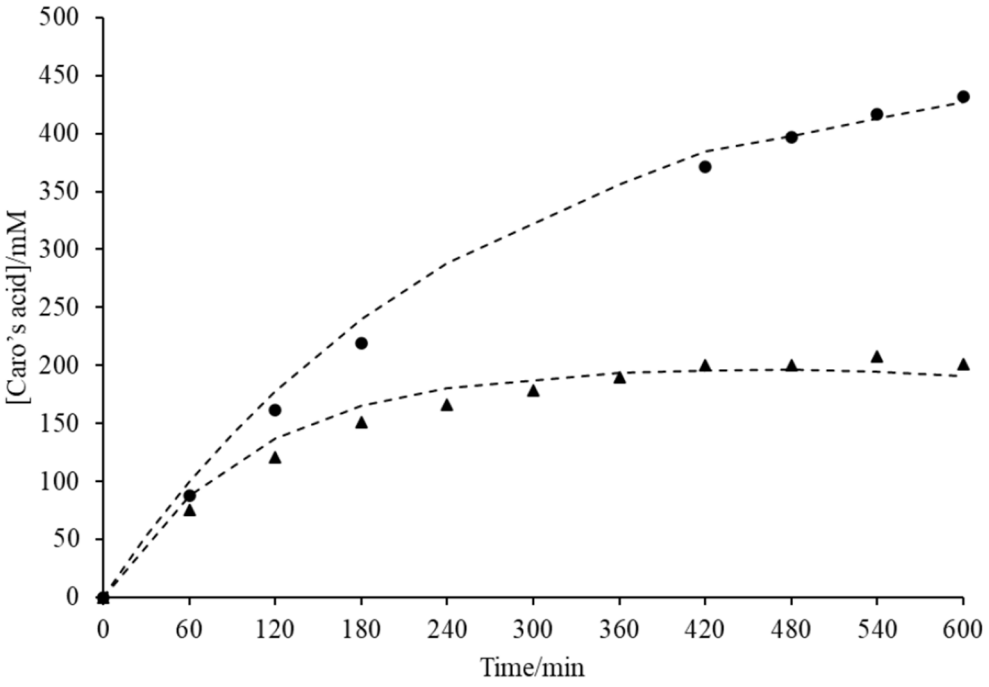

Fig. 6. Electrogeneration of Caro's acid in single compartment (▲) and double (●) compartment, Modelling data dashed line. Current density: 300 mAcm^{-2}, T: 25 °C, electrolyte 1 M H_2SO_4.

Table 1
Phenomenological model for the production of Caro's Acid.

Process/species	S_1 (H_2SO_4)	S_2 (H_2SO_5)	S_3 (H_2O_2)	S_4 (O_2)	Kinetics
Electrochemical production of Caro's acid from sulfuric acid	−1	+1			$\frac{I}{2\cdot F}\eta_{a1}$
Decomposition of Caro's acid	+1	−1		+1	$K_2\cdot[S_2]$
Cathodic formation of hydrogen peroxide			+1	−1	$\frac{I}{2\cdot F}\eta_{c1}$
Chemical production of Caro's acid from hydrogen peroxide	−1	+1	−1		$K_4\cdot[S_1]\cdot[S_3]$
Chemical decomposition of Caro's acid from hydrogen peroxide	+1	−1	−1	+1	$K_5\cdot[S_2]\cdot[S_3]$
Oxygen generation				+1	$\frac{I}{4\cdot F}\eta_{a2}$
Hydrogen generation			+1		$\frac{I}{2\cdot F}\eta_{c2}$

- Single compartment cell: The electrosynthesis of Caro's acid was carried out in a single compartment electrochemical home-designed flow cell made by 3D printing, consisting of two parallel electrodes (5x5 cm) of boron doped diamond (BDD) and stainless steel as anode and cathode, respectively. The interelectrode gap between the electrodes was 6 mm. The experimental setup of the electrolysis system is shown in Fig. 1. Bench scale electrolysis were carried out under galvanostatic conditions and batch (a) and continuous (b) operation mode to determine the influence of the main parameters in the process. The electrolyte consisted in a solution of H_2SO_4 (1 M). A Delta Electronika ES030-10 power supply (0–30 V, 0–10 A) provided the electric current and the applied current densities were within the range of 75–300 mAcm^{-2}. Three temperatures were studied 9 °C, 15 °C and 25 °C. The electrolyte is stored in a dark glass tank (1 dm^3). The electrolyte was circulated through the electrolytic cell by means of a peristaltic pump. A heat exchanger was used to maintain the temperature at desired set point.
- Double compartment cell: A Double compartment electrochemical home-designed cell made by 3D printing was used with Boron doped diamond (BDD) as the anode and stainless steel as cathode. Both electrodes were square plates with a geometric area of (5x5) cm^2. A cationic exchange membrane (Nafion^{TM} 117) was used to separate the compartments. The anolyte and the catholyte were stored in glass tanks (1 dm^3) and they consisted of solutions of sulfuric acid (1 M) circulated through the electrolytic cell by means of a peristaltic pump, as described in Fig. 2. The current density used was 300 mAcm^{-2}. A heat exchanger was used to maintain the temperature at 25 °C.

Table 2
Data of Phenomenological model to produce Caro's Acid.

Operation mode	Anode	Electrolyte	j(mAcm^{-2})	T(°C)	K_2 (s^{-1})	K_4 (s^{-1})	K_5 (s^{-1})	η_1	η_2	r^2
Discontinuous undivided cell	BDD (Nb)	H_2SO_4 (1 M)	300	25	1.57E-04	0.01	0.01	0.8	0.015	0.978
Discontinuous undivided cell	BDD (Nb)	H_2SO_4 (1 M)	300	15	1.23E-04	0.01	0.01	0.8	0.015	0.994
Discontinuous undivided cell	BDD (Nb)	H_2SO_4 (1 M)	300	9	1.23E-04	0.01	0.01	0.8	0.015	0.989
Discontinuous undivided cell	BDD (Nb)	H_2SO_4 (1 M)	150	25	7.38E-05	0.01	0.01	0.8	0.015	0.997
Discontinuous undivided cell	BDD (Nb)	H_2SO_4 (1 M)	75	25	4.82E-05	0.01	0.01	0.8	0.015	0.991
Discontinuous undivided cell	BDD (Nb)	H_2SO_4 (3 M)	300	25	7.82E-05	0.01	0.01	0.8	0.015	0.990
Discontinuous undivided cell	BDD (Nb)	H_2SO_4 (5 M)	300	25	7.42E-05	0.01	0.01	0.8	0.015	0.995
Discontinuous divided cell	BDD (Nb)	H_2SO_4 (1 M)	300	25	6.88E-05	0	0	0.8	0.010	0.995

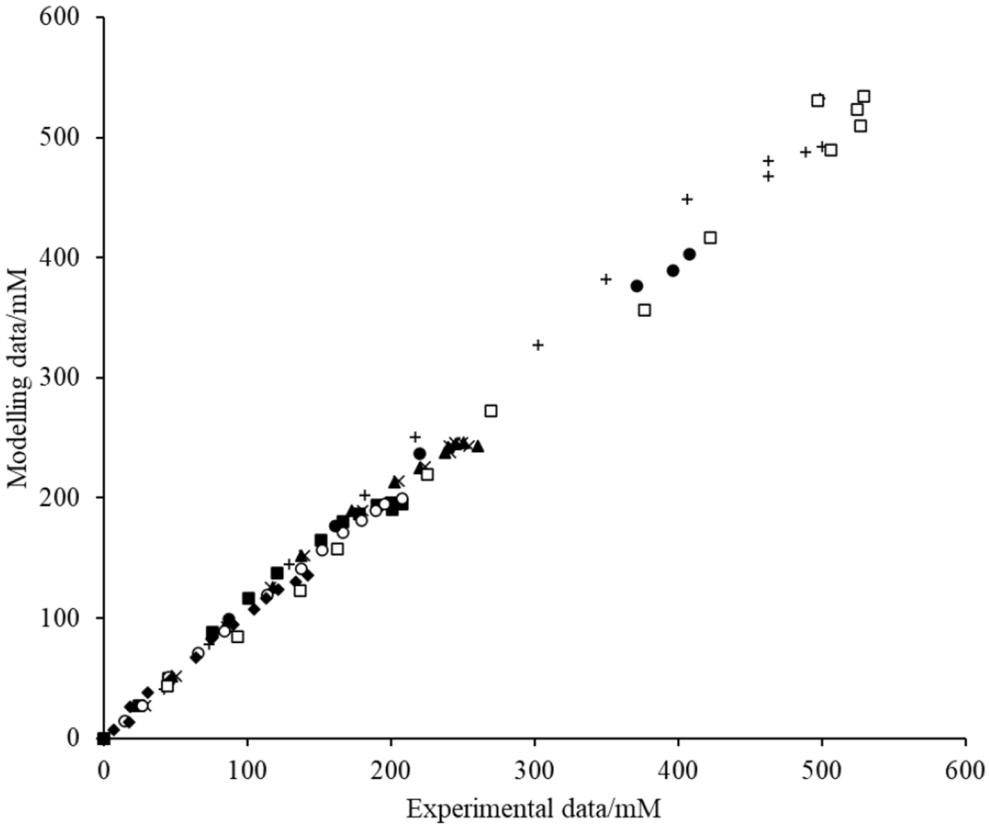

Fig. 7. Model data and experimental data for Caro's acid electrogeneration in batch mode: 300 mAcm^{-2}, 25 °C, 1 M H_2SO_4, single compartment (■);300 mAcm^{-2}, 15 °C, 1 M H_2SO_4, single compartment (○);300 mAcm^{-2}, 9 °C, 1 M H_2SO_4, single compartment (▲);150 mAcm^{-2}, 25 °C, 1 M H_2SO_4, single compartment (×);75 mAcm^{-2}, T 25 °C, 1 M H_2SO_4, single compartment (◆);300 mAcm^{-2}, T 25 °C, 3 M H_2SO_4, single compartment (+);300 mAcm^{-2}, T 25 °C, 5 M H_2SO_4, single compartment (□);300 mAcm^{-2}, T 25 °C, 1 M H_2SO_4, double compartment (●).

3. Results and discussion

Influence of key performance parameters on the discontinuous production of Caro's acid. Electrochemical production of the Caro's acid is a process largely evaluated in the literature, because of the important benefits associated with the production of this oxidant, with many applications not only in industry (e.g. metal finishing) but also in environmental technology (where it is one of the most promising oxidants according to the current scientific literature because it is stable and it can be easily stored and activated) [25,26]. Fig. 3 compares the production of this acid at three different temperatures during electrolysis of 1.0 M sulfuric acid solutions with a pH close to 0.5 at a constant current density.

It points out that very high concentration of the H_2SO_5 can be produced with the new cell equipped with the boron-doped diamond Nb electrode, much higher than typically reported in the literature for similar systems [9,27,28]. The results also show that operating over 20 °C leads to a slight reduction in the efficiency of the processes, which may indicate some sort of thermal decomposition of the oxidant.

However, below this temperature there is no improvement in decreasing temperature, which opposes to the improvement observed when producing electrochemically other oxidants such as ozone or hydrogen peroxide [29]. Both oxidants clearly enhance their electrochemical production when operating at temperatures near 0 °C, because of a prevention in their thermal decomposition [30]. As already known, Caro's acid is thermally stable up to near 60 °C, [1,8] point in which it is known to be decomposed forming sulfuric acid and oxygen according to Eq.5. This observation is very important, because for an industrial production the necessity of cooling is not as relevant as in other electrochemical processes.

$$H_2SO_5^- \rightarrow H_2SO_4 + \frac{1}{2}O_2 \quad (5)$$

Fig. 4 shows the effect of the operation current density on the production of Caro's acid. As seen, this production is speeded up by operating at high current densities. The best current efficiency is obtained at the current density of 150 mA cm^{-2}, indicating that operation at larger current densities may produce higher amounts of oxygen and scavengers. This effect is more clearly observed in the inset of Fig. 4, in which it can be seen that a maximum in the production at this current density, which is more clearly marked as the reaction time increases.

Fig. 5 shows the effect of the concentration of sulfuric acid used as raw matter. Results shown highlight that the efficiency in the production of the Caro's acid is directly related to the concentration of sulfuric acid in the raw matter. Thus, the higher is the concentration of sulfuric acid in the electrolyte, the higher is the concentration for which the peroxymonosulfuric acid is stabilized during the electrolysis made in discontinuous operation mode. However, this improvement in the production of Caro's acid opposites the quality of the final product formed, because of the remaining concentration of sulfuric acid, which is much higher in the case of using highly concentrated sulfuric acid as raw matter.

The ratio between peroxymonosulfuric and sulfuric varies in the final product from 0.25 using the 1.0 M solution down to 0.20 using the 3.0 M solution and to 0.12 mmol H_2SO_5/mmol H_2SO_4 when using the 5.0 M sulfuric acid solution, clearly pointing out that although the production is higher, the dilution into sulfuric acid may make the final product obtained less interesting, because the separation of sulfuric acid and peroxymonosulfuric acid is not a simple challenge. Another important observation regarding the concentration of sulfuric acid in the raw matter comes from cyclic voltammetry. Thus the voltammograms contained in the part b of the Figure show that the peak of the direct formation of peroxymonosulfuric acid (2.0 V vs NHE) is more clearly discerned with the use of higher concentrations of sulfuric acid, which indicates that direct formation of peroxymonosulfuric acid is a primary mechanism with the type of electrodes evaluated, opposite to what it has been stated in the literature regarding the primary role of the hydroxyl radicals in the formation of peroxocompounds, which traditionally have

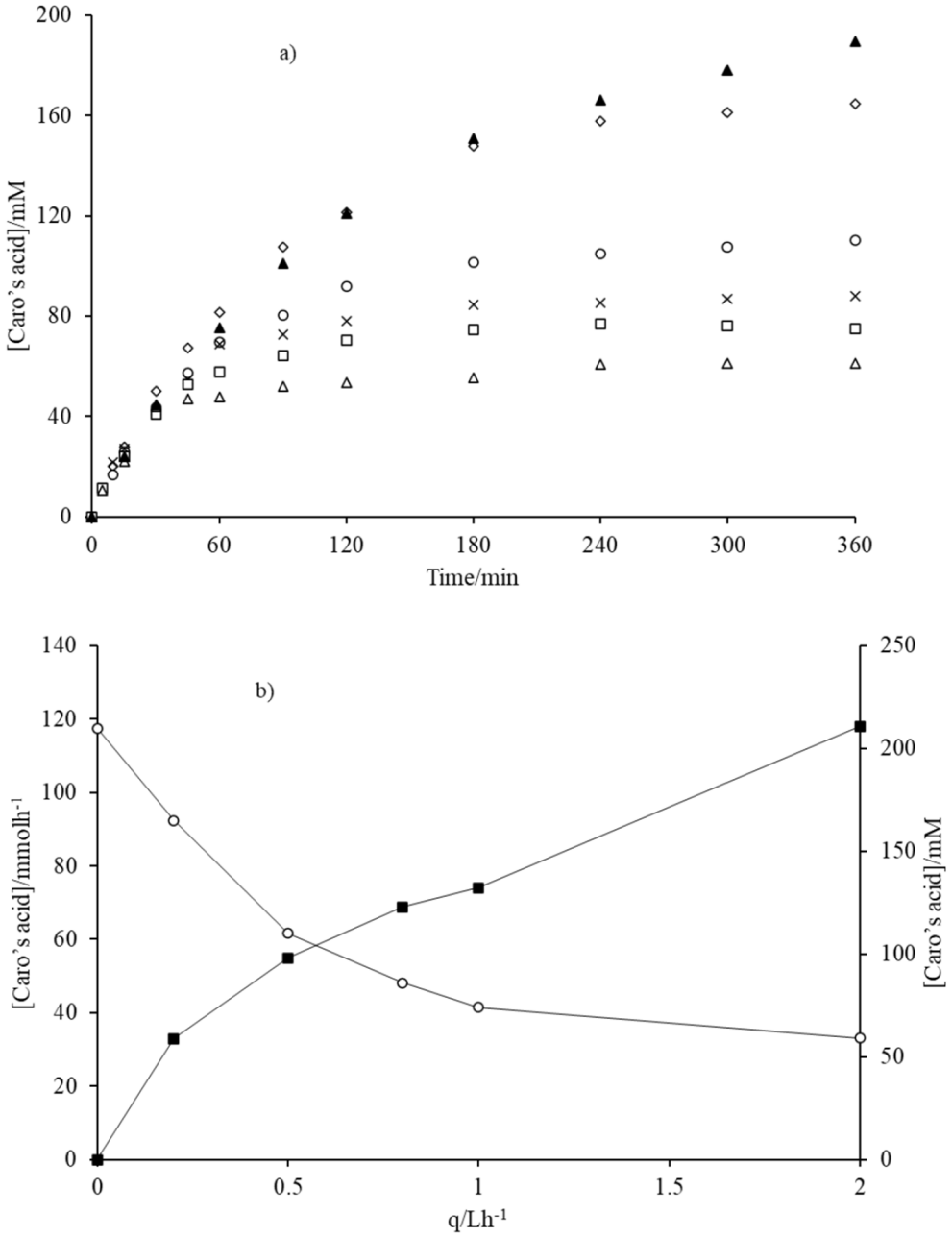

Fig. 8. A) caro's acid electrogeneration in batch (▲) and continuous mode (0.2 lh^{-1} (◊), 0.5 Lh^{-1} (○), 0.8 Lh^{-1} (x), 1.0 Lh^{-1} (□), 2.0 Lh^{-1} ()) in single compartment. Current density: 300 $mAcm^{-2}$, T: 25 °C, electrolyte: 1 M H_2SO_4. b) Caro's acid production (mMh^{-1}) (■) and Caro's acid concentration (mM) at different flow rates (○). Current density: 300 $mAcm^{-2}$, T: 25 °C, electrolyte: 1 M H_2SO_4.

been proposed as the main activators in the formation of these species [31].

Another important point from the operation point of view is the evaluation of the need of compartmentation of the electrochemical cell [32]. As observed in Fig. 6, simply by placing a cationic exchange membrane to separate anodic and cathodic compartments, production of peroxymonosulfuric acid can be more than doubled. Comparison of the first period of the electrolysis (in which decomposition of the Caro's acid is negligible because of its low concentration) indicates that limitations in the production of the oxidant may be related to processes occurring on the cathode or promoted by reductants generated on its surface that becomes Caro's acid scavengers (e.g. hydrogen peroxide). To the knowledge of the authors, the concentration of 400 mM reached here is the highest ever reported for a discontinuous operated electrochemical production of Caro's acid and means the production of a really impressive product with a ratio 0.76 mmol H_2SO_5/mmol H_2SO_4 without any further purification.

Phenomenological model for the electrochemical production of Caro's acid. To better understand the production of the Caro's acid a simple phenomenological model is proposed (Table 1).

This model takes into account that only two reactions will occur on the anode surface, namely the formation of Caro's acid (process 1) and the evolution of oxygen (process 6). Thus, η_{a1} represents the percentage of the current used in process 1, while η_{a2} represents the percentage of current used in process 2. Given that no other processes are considered, the sum of both parameters is 1. Concerning the cathodic process, the model posits that hydrogen peroxide (process 3) and hydrogen (process 7) are the only reactions that may occur on the cathode surface. The percentages of current (coulombic efficiency) for these processes are $\eta c1$ and η_{c2}, respectively, and their sum is also 1. The model considers three

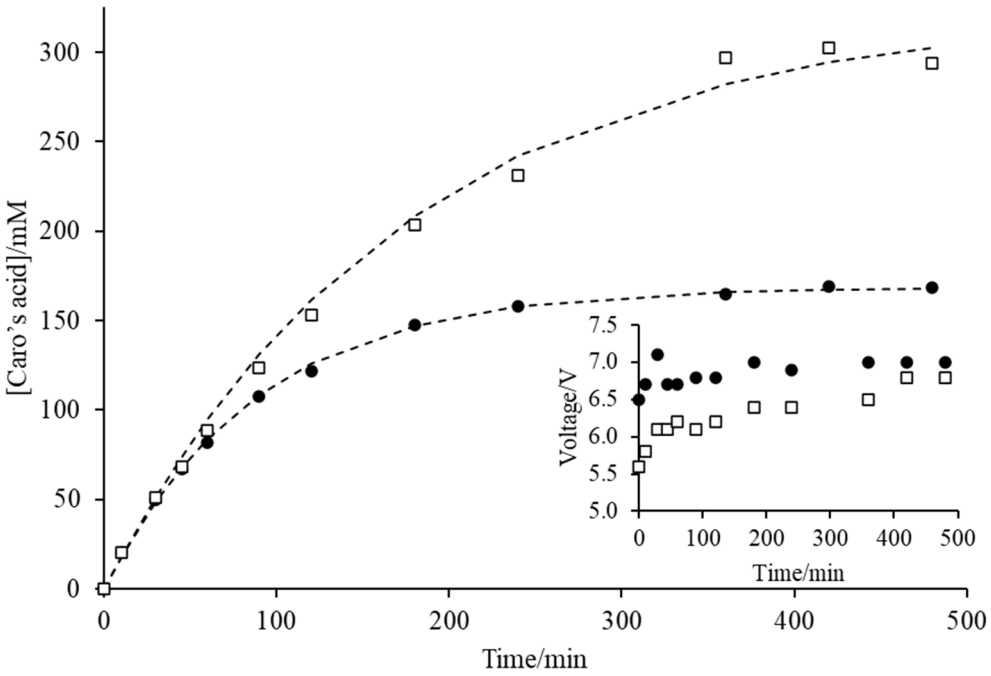

Fig. 9. Comparison of the production of Caro's acid in single (●) and double (□) compartment electrochemical cell operated in continuous mode. Insert: cell voltage.

chemical processes: the chemical decomposition of Caro's acid to generate oxygen and sulfuric acid (K_2), which varies depending on the conditions of temperature, current density, and electrolyte concentration (Table 2); and the interaction of sulfuric acid and Caro's acid with hydrogen peroxide (processes 4 and 5, respectively), for which simple chemical kinetic expressions are also provided (K_4 and K_5).

The Petersen stoichiometric and kinetic matrix is shown in Table 1, where the sum of anodic and cathodic efficiencies is equal to 1, respectively.

Experimental data shown in the previous section were fitted to the model and the lines plotted are the simulation values calculated with the model. As seen the model reproduces satisfactorily all results obtained with regression coefficients over 0.97 shown in Table 2 in every case and in which the values of the kinetic constants are almost fixed for all conditions, pointing out the robustness of the approaches made.

This can also be clearly seen in the plot model vs experimental data shown in Fig. 7 which fits almost perfectly to the line $y_{modelled} = y_{experimental}$.

Operation in continuous mode. Once clarified the role of the different inputs in the electrochemical production of Caro's acid and considering that the key limitation in the production is the decomposition of the oxidant, which depends importantly on concentration, it is clear that operation in continuous mode can help to face this limitation by purging the peroxymonosulfuric acid continuously preventing its decomposition in the electrochemical cell. Fig. 8 shows the changes in the concentration of peroxymonosulfuric acid during discontinuous electrolysis at 300 mA cm^{-2} and during electrolysis performed in continuous mode at different flow rates (from 2 and 0.2 Lh^{-1} corresponding to residence time ranging from 30 to 300 min). As it can be seen, concentration stabilizes in all of them, although the cause is completely different. In continuous process the stabilization is not only explained in terms of the balance between the rates of formation and decomposition of the oxidant but because the oxidant produced is continuously removed from the system. Thus, production in the discontinuous system is obtained as the product of the concentration stabilized and the volume of electrolyte and it reaches the final value after a given operation time, while in continuous processes the production is the product flowrate by the stabilization concentration and hence, it is much higher. However, the higher is the flowrate the lower will be the concentration of Caro's acid in the product as can be seen in part b of the Fig. 8.

Going further in the optimization of the production, the use of membranes to separate anodic and cathodic processes may help to improve the performance of the system as it did in the discontinuously operated process. Fig. 9 shows the transient response up to the stabilization during the continuous electrolysis at a flowrate of 0.2 Lh^{-1}. As seen the production can be more than doubled while the cell voltage increases only by a factor of 10 %. This means that it is worth to use the membranes and that total production is 58.8 mmol/h vs 33 mmol/h which means real global efficiencies (discounting degradation processes of the peroxymonosulfuric acid) of nearly 42.03 and 23.58 %, respectively.

Considering the cell voltage and the intensity applied the power consumed is 52.5 W (7.0 V· 7.5 A) in the case of the two-compartment cell and 51 W (6.8 V · 7.5 A) in the case of the one compartment cell. This means that in double compartment cell the cost is 1.12 mmol/Wh which is a really promising operation cost.

4. Conclusions

From this work, the following conclusion can be drawn:

- Caro's acid can be efficiently produced using BDD electrodes and a novelty tailored 3D-printed reactor Among the different parameters studied, decreasing temperature to 10 °C respect to 25 °C, has demonstrated a positive impact on Caro's acid generation (250 mM vs 200 mM, respectively), and increasing the sulfuric acid concentration used as raw matter from 1 to 3 M increases notably the production of Caro's acid, from 200 mM to 500 mM respectively, proving that both a high acidic environment and more raw material favor its production. Finally, a moderate 150 mA·cm-2 current density presents the better results for current efficiency, showing that a compromise between reaching the optimal cell potential to produce the Caro's acid and a moderate degradation on the cathode must be reached.
- The production of Caro's acid in a two-compartment cell far exceeds (more than double (430 mM)) the production in one compartment cell. These data proves that Caro's acid undergo a massive cathodic

degradation when working in single compartment, thus acting as the limiting factor for its production. A two-compartment cell is necessary for applications that needs a more concentrated product or for mass-production and storage of Caro's acid.

- A phenomenological model allows to fully understand and predict the generation of Caro's acid using BDD electrodes by considering the efficiency of the formation of Caro's acid and hydrogen peroxide and the different ways in which Caro's acid can undergo decomposition. This model can fit the experimental data obtained and will help to further predict the behavior of the system for further scaling purposes.
- The feasibility of the continuous generation of Caro's acid has been demonstrated for different flow rates and one-two compartment electrochemical cells. Controlling the flow rate is possible to adjust the Caro's acid concentration output and production, being an extremely useful tuning tool to adapt to any application.

CRediT authorship contribution statement

M.P. Castro: Investigation, Data curation, Formal analysis, Writing – original draft. **I.F. Mena:** Investigation, Writing – original draft. **M.A. Montiel:** Investigation, Writing – review & editing. **J. Gäbler:** Validation, Writing – review & editing. **L. Schäfer:** Validation, Supervision, Writing – review & editing. **C. Sáez:** Validation, Supervision, Writing – review & editing. **M.A. Rodrigo:** Conceptualization, Funding acquisition, Project administration, Supervision, Validation, Writing – review & editing.

Declaration of Competing Interest

The authors declare that they have no known competing financial interests or personal relationships that could have appeared to influence the work reported in this paper.

Data availability

The authors do not have permission to share data.

Acknowledgements

This work comprises the research project PCI2021-121963 granted by MCIN/ AEI/10.13039/501100011033/ and "Unión Europea Next-GenerationEU/PRTR". Miguel A. Montiel e Ismael F. Mena thanks funding received through the excellence program Juan de la Cierva Formación FJC2019-039279-I and FJC2019-039962-I, respectively. The authors would like to thank the EU and Bundesministerium für Bildung und Forschung, Germany, Ministero dell'Università e della Ricerca, Italy, Agencia Estatal de Investigación, Spain, Fundação para a Ciência e a Tecnologia, Portugal, Norges forskningsråd, Norway, Water Research Commission, South Africa for funding, in the frame of the collaborative international consortium SERPIC financed under the ERA-NET AquaticPollutants Joint Transnational Call (GA N° 869178). This ERA-NET is an integral part of the activities developed by the Water, Oceans and AMR Joint Programming Initiatives.

Appendix A. Supplementary material

Supplementary data to this article can be found online at https://doi.org/10.1016/j.seppur.2023.124118.

References

[1] K.G. Serrano, A critical review on the electrochemical production and use of peroxo-compounds, Curr. Opin. Electrochem. 27 (2021), 100679.
[2] G. Divyapriya, P. Nidheesh, Electrochemically generated sulfate radicals by boron doped diamond and its environmental applications, Curr. Opin. Solid State Mater. Sci. 25 (2021), 100921.
[3] Y. Chen, P. Deng, P. Xie, R. Shang, Z. Wang, S. Wang, Heat-activated persulfate oxidation of methyl- and ethyl-parabens: effect, kinetics, and mechanism, Chemosphere 168 (2017) 1628–1636.
[4] S. Dhaka, R. Kumar, M.A. Khan, K.-J. Paeng, M.B. Kurade, S.-J. Kim, B.-H. Jeon, Aqueous phase degradation of methyl paraben using UV-activated persulfate method, Chem. Eng. J. 321 (2017) 11–19.
[5] F. Pardo, A. Santos, A. Romero, Fate of iron and polycyclic aromatic hydrocarbons during the remediation of a contaminated soil using iron-activated persulfate: a column study, Sci. Total Environ. 566 (2016) 480–488.
[6] Y. Ji, Y. Fan, K. Liu, D. Kong, J. Lu, Thermo activated persulfate oxidation of antibiotic sulfamethoxazole and structurally related compounds, Water Res. 87 (2015) 1–9.
[7] J. Davis, J.C. Baygents, J. Farrell, Understanding persulfate production at boron doped diamond film anodes, Electrochimica Acta 150 (2014) 68–74.
[8] J. Cai, M. Zhou, Y. Liu, A. Savall, K.G. Serrano, Indirect electrochemical oxidation of 2, 4-dichlorophenoxyacetic acid using electrochemically-generated persulfate, Chemosphere 204 (2018) 163–169.
[9] K.C. Araújo, K.N. Silva, M.K. Monteiro, D.R. da Silva, M.A. Quiroz, E.V. dos Santos, C.A. Martínez-Huitle, Towards use of persulfate electrogenerated at boron doped diamond electrodes as Ex-situ oxidation approach: storage and service-life solution parameters, J. Electrochem. Soc. 169 (2022), 033506.
[10] M. Josef, B. Franz, Evonik Degussa GmbH, Process for the production of caro's acid salts and solutions thereof. United States patent US 3,036,885. 1962.
[11] E.T. Fell, Stevensons Dyers Ltd, Process for making peroxymonosulphuric acid. United States patent US 2,789,954. 1957.
[12] K.C. de Freitas Araujo, D.R. da Silva, E.V. dos Santos, H. Varela, C.A. Martínez-Huitle, Investigation of persulfate production on BDD anode by understanding the impact of water concentration, J. Electroanalytical Chem. 860 (2020), 113927.
[13] K. Serrano, P. Michaud, C. Comninellis, A. Savall, Electrochemical preparation of peroxodisulfuric acid using boron doped diamond thin film electrodes, Electrochimica Acta 48 (2002) 431–436.
[14] S. Bebelis, K. Bouzek, A. Cornell, M.G.S. Ferreira, G.H. Kelsall, F. Lapicque, C.P. de Leon, M.A. Rodrigo, F.C. Walsh, Highlights during the development of electrochemical engineering, Chem. Eng. Res. Des. 91 (2013) 1998–2020.
[15] C.A. Martínez-Huitle, M.A. Rodrigo, I. Sirés, O. Scialdone, A critical review on latest innovations and future challenges of electrochemical technology for the abatement of organics in water, Appl. Catal. B 328 (2023), 122430.
[16] K.C.F. Araújo, E.V. dos Santos, P.V. Nidheesh, C.A. Martínez-Huitle, Fundamentals and advances on the mechanisms of electrochemical generation of persulfate and sulfate radicals in aqueous medium, Curr. Opin. Chem. Eng. 38 (2022), 100870.
[17] B.-T. Zhang, Y. Zhang, Y. Teng, M. Fan, Sulfate radical and its application in decontamination technologies, Crit. Rev. Environ. Sci. Technol. 45 (2015) 1756–1800.
[18] J. Yao, Y. Zhang, Z. Dong, Enhanced degradation of contaminants of emerging concern by electrochemically activated peroxymonosulfate: performance, mechanism, and influencing factors, Chem. Eng. J. 415 (2021), 128938.
[19] M. Rodriguez-Pena, J.A.B. Perez, J. Llanos, C. Saez, C.E. Barrera-Diaz, M. A. Rodrigo, Toward real applicability of electro-ozonizers: Paying attention to the gas phase using actual commercial PEM electrolyzers technology, Chemosphere 289 (2022).
[20] M. Rodriguez-Peña, J.B. Pérez, J. Llanos, C. Saez, C.E. Barrera-Díaz, M.A. Rodrigo, Electrochemical generation of ozone using a PEM electrolyzer at acidic pHs, Sep. Purif. Technol. 267 (2021), 118672.
[21] G. Acosta-Santoyo, L.F. Leon-Fernandez, E. Bustos, P. Canizares, M.A. Rodrigo, J. Llanos, On the production of ozone, hydrogen peroxide and peroxone in pressurize d undivide d electrochemical cells, Electrochimica Acta 390 (2021).
[22] I. Kolthoff, E. Carr, Volumetric determination of persulfate in presence of organic substances, Anal. Chem. 25 (1953) 298–301.
[23] G. Eisenberg, Colorimetric determination of hydrogen peroxide, Ind. Eng. Chem. Anal. Ed. 15 (1943) 327–328.
[24] L. Schäfer, M. Höfer, R. Kröger, The versatility of hot-filament activated chemical vapor deposition, Thin Solid Films 515 (2006) 1017–1024.
[25] I. Moraleda, S. Cotillas, J. Llanos, C. Saez, P. Canizares, L. Pupunat, M.A. Rodrigo, Can the substrate of the diamond anodes influence on the performance of the electrosynthesis of oxidants? J. Electroanalytical Chem. 850 (2019).
[26] P. Canizares, C. Saez, A. Sanchez-Carretero, M.A. Rodrigo, Synthesis of novel oxidants by electrochemical technology, J. Appl. Electrochem. 39 (2009) 2143–2149.
[27] I. Moraleda, S. Cotillas, J. Llanos, C. Sáez, P. Cañizares, L. Pupunat, M.A. Rodrigo, Can the substrate of the diamond anodes influence on the performance of the electrosynthesis of oxidants? J. Electroanalytical Chem. 850 (2019), 113416.
[28] P.A. Michaud, E. Mahé, W. Haenni, A. Perret, C. Comninellis, Preparation of peroxodisulfuric acid using boron-doped diamond thin film electrodes, Electrochem. Solid St. 3 (1999) 77.
[29] M. Rodriguez-Pena, J.A.B. Perez, J. Llanos, C. Saez, C.E. Barrera-Diaz, M. A. Rodrigo, Understanding ozone generation in electrochemical cells at mild pHs, Electrochimica. Acta. 376 (2021).
[30] M.K. Sales Monteiro, Á. Moratalla, C. Sáez, E.V. Dos Santos, M.A. Rodrigo, Electrochemical production of hydrogen peroxide in perchloric acid supporting

electrolytes for the synthesis of chlorine dioxide, Ind. Eng. Chem. Res. 61 (2022) 3263–3271.
[31] P. Canizares, C. Saez, J. Lobato, R. Paz, M.A. Rodrigo, Effect of the operating conditions on the oxidation mechanisms in conductive-diamond electrolyses, J. Electrochem. Soc. 154 (2007) E37–E44.
[32] C.A. Martínez-Huitle, M.A. Rodrigo, I. Sirés, O. Scialdone, Single and coupled electrochemical processes and reactors for the abatement of organic water pollutants: a critical review, Chem. Rev. 115 (2015) 13362–13407.